Fluid Suspensions of Colloidal Ellipsoids: Direct Structural Measurements

A. P. Cohen,[1] E. Janai,[1] E. Mogilko,[1] A. B. Schofield,[2] and E. Sloutskin[1,*]

[1]*Physics Department and Institute for Nanotechnology and Advanced Materials, Bar-Ilan University, Ramat-Gan 52900, Israel*

[2]*The School of Physics and Astronomy, University of Edinburgh, Edinburgh EH9 3JZ, United Kingdom*

(Received 23 June 2011; published 2 December 2011)

A fluid of spheroids, ellipsoids of revolution, is among the simplest models of the disordered matter, where positional and rotational degrees of freedom of the constituent particles are coupled. However, while highly anisometric rods, and hard spheres, were intensively studied in the last decades, the structure of a fluid of spheroids is still unknown. We reconstruct the structure of a simple fluid of spheroids, employing direct confocal imaging of colloids, in three dimensions. The ratio t between the polar axis and the equatorial diameter for both our prolate and oblate spheroids is not far from unity, which gives rise to a delicate interplay between rotations and translations. Strikingly, the measured positional interparticle correlations are significantly stronger than theoretically predicted, indicating that further theoretical attention is required, to fully understand the coupling between translations and rotations in these fundamental fluids.

DOI: 10.1103/PhysRevLett.107.238301 PACS numbers: 82.70.Dd, 05.20.Jj, 07.60.Pb, 47.57.J−

During recent decades, significant scientific interest has focused on fundamental studies of simple fluids, composed of spherical particles [1–3]. However, much of the rich behavior of real atoms and molecules stems from their spherically anisotropic shapes and interaction potentials [4]; perfect spheres are inappropriate as a model for these systems. The thermodynamical state of a fluid of particles interacting through short-range repulsions, is determined by the amount of free volume, which is available for each individual particle; this free volume, for spheroids, is a nonanalytic function of the aspect ratio [5] t, for $t = 1$. Thus, the fluid structure may possibly exhibit a similar nonanalyticity; this suggests that the collective behavior of nearly spherical ellipsoids is different from that of the simple spheres. Several theoretical models [6–9] have been suggested in recent decades to describe fluids of ellipsoidal particles. However, direct experimental structural studies of dense bulk [10] fluids of ellipsoids, with the positions and the orientations of individual particles resolved, are still absent [11,12]. Thus, the structure of these basic and fundamental fluids remains obscure.

We form a dense fluid of ellipsoids, with an aspect ratio of $t = 1.6$ and measure its structure, detecting the real-space positions of all particles in motion, in three spatial dimensions. We quantify the short-range structure and correlations in our fluids, employing the experimental radial distribution function [2] $g(R)$. These $g(R)$, obtained at several different particle densities, demonstrate that the positional correlations in our system are much more pronounced than theoretically predicted. Moreover, we observe a similar increase in positional correlations also for the oblate $t \approx 0.25$ spheroids. We demonstrate that the increased positional correlations result from coupling between the rotational and the positional degrees of freedom. This coupling does not exist for the spheres; also, for large t, the rotational degrees of freedom dominate, such that translations and rotations are, effectively, decoupled. In our range of moderate t, neither the rotational nor the positional degrees of freedom can dominate, which gives rise to a rather complex interplay, beyond common theoretical models.

Colloids, micron-sized particles in a molecular solvent, undergo Brownian motion, such that their free energy is minimized; thus, colloidal suspensions mimic the collective behavior of atoms and molecules. Colloids are sufficiently large for optical microscopy; this allows their behavior to be studied in great detail by confocal microscopy, which provides far more precise information, compared to other experimental techniques. We employ the Nikon A1R resonant laser-scanning confocal system, to image thousands of fluorescently labeled colloidal particles in real time, within the bulk of a truly macroscopic sample, where size effects are entirely negligible.

To form our prolate ellipsoids (PE), we suspend PMMA [poly(methyl methacrylate)] colloidal spheres, of diameter $\sigma = 2.4$ μm, in a solution of PDMS [poly(dimethylsiloxane)], which is then crosslinked [12]; our initial spheres are sterically stabilized by polyhydroxystearic acid (PHSA), and fluorescently labeled by the Nile red dye, for confocal microscopy. We stretch the crosslinked PDMS films, with the particles embedded inside, by a factor of 1.37, at $T = 180\,^{\circ}$C, where particles are soft, employing a computerized stretching device. Our device allows the stretching process to be sufficiently slow, uniform, and accurate, to avoid film tearing, and to minimize the shape polydispersity of the resulting ellipsoids [12]. The particles, stretched to an aspect ratio of $t = 1.6$, are released by chemical destruction of PDMS [12]. To measure the shape of our particles, we deposit them from mixed-decahyrdonaphthalene (Sigma-Aldrich, $\geq 98\%$) onto a silicon substrate, and obtain scanning electron microscopy (SEM) images [at 30 keV, see Fig. 1(a)]. The apparent

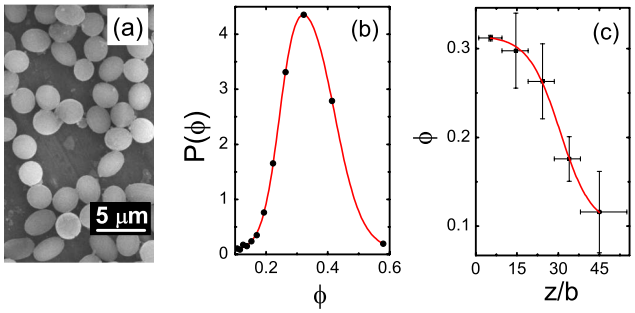

FIG. 1 (color online). (a) SEM image of our prolate ellipsoids. (b) The experimental probability distribution for the local volume fraction values ϕ (solid symbols), at a given height z above the bottom of the sample, is fitted (red curve) by an asymmetric double sigmoidal function, which is roughly Gaussian. A typical thermodynamically stable density profile $\phi(z)$, obtained from the peak positions of $P(\phi)$, is shown in (c); the red curve is a guide to the eye. The z regions, used in the analysis, are marked by horizontal error bars; the vertical error bars show the variations between our samples.

average aspect ratio in these images $t_s = 1.34$ corresponds to the projection of our particles onto the surface of the silicon substrate; t_s sets the bottom limit for t, as some of the particles may have their long axes oriented at a nonzero angle to the substrate. If all our particles are randomly oriented with respect to the substrate, their actual aspect ratio must be larger, $t_r \approx 1.9$. The surface-parallel orientation minimizes surface energy, while all other orientations can only be metastable; thus, the surface-parallel orientation is, on average, more likely than all other orientations, such that t_r sets the upper limit on t. In addition, we confirm the aspect ratio of our ellipsoids by confocal microscopy.

To thermalize our ellipsoids, we suspend them in a mixture (18:22:60, by mass) of cis-decahydronaphthalene (Fluka, $\geq 98\%$), tetrahydronaphthalene (Sigma-Aldrich, $\geq 99\%$) and tetrachloroethylene (Sigma-Aldrich, $\geq 99.5\%$). Our particle preparation process damages parts of the steric PHSA layer [13]; to stabilize our particles by short-ranged screened Coulombic repulsions [14], we introduce 70 mM aerosol OT (AOT, or dioctyl sodium sulfosuccinate, Sigma-Aldrich, $\geq 98\%$) to the suspension. Our mixed solvent matches the refractive index of the particles, which allows confocal imaging deep into the bulk of the samples. In addition, the density of our solvent is only slightly lower than the gravimetric density of our particles, such that the sedimentation, in the field of gravity, is balanced by the osmotic pressure. Thus, the particles form a stable density profile within the capillary, which does not change on a scale of several weeks, indicating that thermodynamical equilibrium was attained.

To reconstruct the structure of the fluid, we collect a stack of confocal slices through the sample, using a $100x$ oil-immersion objective. Our voxel size $0.08 \times 0.08 \times 0.3\ \mu\text{m}^3$ slightly oversamples beyond the optical resolution of $0.11 \times 0.11 \times 0.34\ \mu\text{m}^3$; this improves the accuracy of the particle tracking algorithm, which is based on the PLuTARC code [15], generalized here for tracking of ellipsoids. A two-dimensional slice through an ellipsoidal particle is an ellipse. The algorithm first detects the centers and orientational angles of all such ellipses, in each of the two-dimensional confocal slices. Then, the code links between centers of ellipses, which belong to adjacent slices, based on the lateral separation and the orientation of these ellipses; this provides the (x, y, z) coordinates of the center of each ellipsoid in our system.

To determine the local volume, which is available for each individual particle, we perform Voronoi tessellation [16] of our sample; the Voronoi cell of the ith particle is the locus of all points, which are located closer to the center of this particle, than to any other particle in the system. To estimate the local volume fraction of the colloids ϕ, we divide the single-particle volume $v = \pi b^3 t/6$ by the volume of its Voronoi cell, where $b = 2.1\ \mu\text{m}$ is the short axis of our PE. The probability of observing a certain value of ϕ in our system is almost perfectly Gaussian, as shown in Fig. 1(b); this is typical for fluids at low density, far from the glass transition [2]. The peak position of this distribution corresponds to the average volume fraction ϕ at a certain height z above the bottom of the sample. Thus, $\phi(z)$ measures the density profile of colloids, which is determined by the balance between gravity and osmotic pressure [17]; a typical $\phi(z)$ is shown in Fig. 1(c). The structure of the fluid at a given height is fully determined by the local value of $\phi(z)$. Thus, each single sample with a thermodynamically stable density profile, allows the fluid structure for a range of densities to be measured.

To quantify the local structure of the fluid of PE, we obtain the radial distribution function $g(r)$, which is proportional to the probability of finding two particles, with their centers separated by a distance r; this function is normalized such that it is equal to 1 for an ideal gas, where particles are uncorrelated. Our particles do not interpenetrate; thus, $g(r)$ is identically zero for $r < b$; see Figs. 2(a) and 2(b), where the experimental $g(r)$, at two different volume fractions, are shown in solid symbols. The peaks of $g(r)$ correspond to the coordination shells, which surround each particle in the fluid. Fluids are characterized by short-range, exponentially decaying, positional correlations between the constituent particles; thus, for high r, the coordination shells are totally smeared by thermal fluctuations, such that $g(r) = 1$, as in the ideal gas. The rotational anisotropy of our ellipsoids may, naively, be expected to smear the shell structure of the fluid; however, the 3rd and the 4th coordination shells are clearly distinguishable in the experimental $g(R)$. This indicates that non-negligible positional correlations are present; these correlations increase with the volume fraction ϕ, which is typical for simple fluids [2].

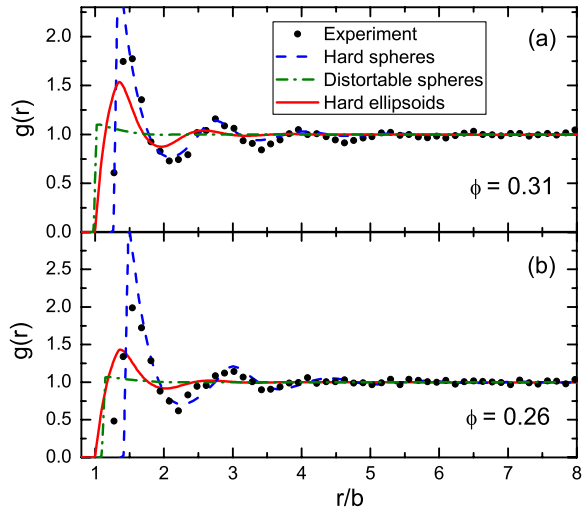

FIG. 2 (color online). The experimental radial distribution function $g(r)$ of PE (solid symbols), is shown for (a) $\phi = 0.31$ and (b) $\phi = 0.26$; r is normalized by the short axis of our ellipsoids b. The simple hard spheres model (blue dashes) matches the experimental data, albeit for an unreasonable set of free parameters. A more advanced model [9] (olive dash-dotted curve), describing our particles, as if these were entrapped in distortable spheres, such that their rotational degrees of freedom are not completely neglected, is in very poor agreement with the experimental $g(r)$, indicating that the coupling between rotational and positional degrees of freedom must be explicitly taken into account. The $g(r)$ obtained by such explicit calculation [7] (solid red curve), is closer to the experimental data; yet, this model significantly underestimates the extent of positional correlations.

Our PE are only slightly anisotropic; thus, this anisotropy may be considered a small perturbation, with respect to the well-known fluid of simple hard spheres. To better understand the full shape of our experimental $g(r)$, we fit to it the theoretical $g(r)$ of hard spheres, obtained in the well-known Percus-Yevick approximation [2]; to have the theoretical curve match our experimental data, we set both the diameter of the theoretical (effective) spheres, and their volume fraction, as free parameters. Remarkably, as also in earlier x-ray scattering studies of nonspherical particles [11], which involved multiple free parameters and rather nontrivial approximations, a good match is found between the theoretical curves and the experimental data, at all experimental ϕ, as shown in Figs. 2(a) and 2(b). The fitted diameter and volume fraction of the effective hard spheres are higher than the experimental ones. For example, to fit the data in Fig. 2(a), we had to set the diameter of the effective hard spheres to $\sigma_{\text{eff}} = 2.7\ \mu$m, while their volume fraction is set to $\phi_{\text{eff}} = 0.4$. This value of σ_{eff} is higher than σ, the diameter of our initial spheres, which we have stretched into ellipsoids, subject to volume preservation; thus, the anisotropy of our particles, albeit very small, changes the fluid structure in a nontrivial way. Unfortunately, the exact interpretation of the fitted values of σ_{eff} and ϕ_{eff} is not clear; in particular, $\phi_{\text{eff}} = 0.4$ in both Figs. 2(a) and 2(b), while the actual volume fraction of the experimental ellipsoids grows by almost 20%. This discouraging behavior of ϕ_{eff} is hardly surprising; the effective hard spheres model neglects all orientational correlations which may exist in our system, where positional and rotational degrees of freedom are coupled. In particular, this theoretical model assumes that the likeliest distance between the particles is independent of their volume fraction ϕ_{eff}; this is in contrast with the real-life ellipsoids, where nearest neighbors (NNs) can assume roughly parallel orientations, to decrease the distance between their centers of mass. Recently, a very simple theoretical model [9] was suggested to account for this effect. This model regards the ellipsoids, as if they were entrapped inside effective spheres, which, at very low ϕ, allow free rotation. The spheres shrink with ϕ, which accounts for the increase in local orientational correlations between the actual ellipsoidal particles. This simple argumentation was recently shown [9] to exactly reproduce the structure of a fluid of highly anisometric colloids, where the rotational degrees of freedom are effectively frozen [18]. However, for the very modest aspect ratio of our PE, the interplay between rotations and translations is far more intricate, such that the current model totally fails to reproduce the experimental $g(r)$, as shown in the dash-dotted curve, in Figs. 2(a) and 2(b). Thus, a more accurate treatment of the correlations between rotations and translations is necessary.

To directly account for the coupling between rotations and translations, we adopt an explicit solution for ellipsoids [7] of the Ornstein-Zernike equation, in the Percus-Yevick (PY) approximation [2,3]. This model, albeit approximate, is in a good agreement with computer simulations of ellipsoids [8,19–21]. On a qualitative level, the resulting function, shown in Figs. 2(a) and 2(b) (in solid red line), reproduces all features observed in the experimental $g(r)$. Yet, strikingly, these theoretical $g(R)$ significantly underestimate the positional correlations in our system, as the oscillations in $g(r)$ decay much faster, than experimentally observed. This discrepancy cannot be eliminated by tuning b, ϕ, and t to any reasonable value [14].

To further test the generality of our results, we form a fluid of oblate ellipsoids (OE), such that $t \approx 0.25$. For that purpose, we compress our PDMS films under load, instead of stretching them; the sample preparation is, otherwise, the same as above. Unfortunately, our oblate ellipsoids are not as monodisperse, in terms of their aspect ratio, as the PE. The $g(r)$ for the OE are shown in Fig. 3, together with the theoretical fits. Strikingly, while the model of effective hard spheres matches nicely the experimental data, the explicit PY theory of hard ellipsoids [7] significantly underestimates the extent of positional correlations in our system; this is even more surprising, in view of the shape

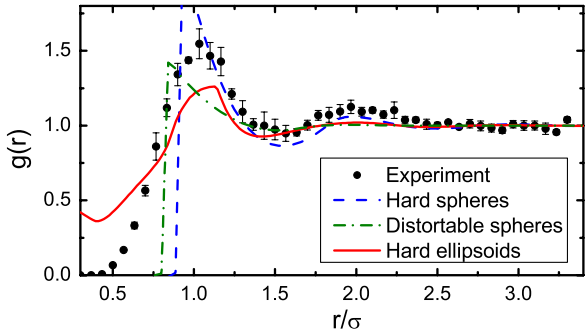

FIG. 3 (color online). The experimental $g(r)$ of our oblate ellipsoids ($t \approx 0.25$) at $\phi \approx 0.35$; here $\sigma = 2.4$ μm is the diameter of our original spheres. The symbols are the same as in Fig. 2. The r of the solid curve, in σ units, was divided by a factor [14] of 1.4, to improve the match with the experimental data.

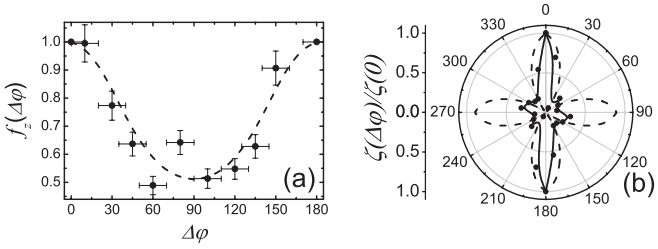

FIG. 4. The PY theory (dashes) for the prolate ellipsoids matches, with no free parameters, the experimental (symbols) depletion of NN particles, which have their azimuths oriented at $\Delta\varphi$ to each other, as shown in (a). However, $\zeta(\Delta\varphi)/\zeta(0)$, which is a more sensitive measure of the orientational correlations, indicates that the theory overestimates the experimental orientational correlations between the NNs for $\Delta\varphi = 90°$, as shown in (b). The solid curve is a B spline through the experimental data.

polydispersity of our OE, which is expected to diminish correlations. Thus, even in a very simple fluid of spheroids, the positional correlations are significantly underestimated by the common theoretical models, for both oblate and prolate particles. This discrepancy is in contrast with the perfect agreement between experimental $g(r)$ and PY predictions, for colloidal hard spheres [1]; thus, it is the coupling with the rotational correlations, which must be responsible for the observed discrepancy. In particular, a possible overestimate of the orientational correlations may increase the theoretical free volume available for particle translations; this would diminish the theoretical positional correlations, compared to the experimental ones.

To test this hypothesis, we directly measure the orientations of our PE. The orientation of each particle is determined, in the lab frame, by two angles, θ and φ. We choose θ to be the inclination with respect to the optical axis of the microscope; φ is the azimuth. We measure the radial distribution function $g(r, \Delta\varphi)$ of particles, within an optical slice through the system, which have the difference between their azimuths $\Delta\varphi$ fixed at a certain value. At small r, parallel orientations of NNs are more likely. The abundance of NNs which have an angle $\Delta\varphi$ between their azimuths, normalized by the abundance of NNs which both have identical azimuths $f_z(\Delta\varphi) = (r' - b)^{-1} \int_b^{r'} g(r, \Delta\varphi)/g(r, 0)dr$ is shown in Fig. 4(a). Interestingly, these data are in perfect agreement with the PY theoretical prediction for the PE [7,22], obtained with no free parameters; here, arbitrarily, $r' = 1.3b$. Thus, the theoretical coupling between rotations and translations matches the experimentally observed one. To measure the orientational correlations in a more delicate way, we define $\zeta(\Delta\varphi) = \int [g(r, \Delta\varphi)/g(r) - 1]^2 dr$, where $g(r)$ is the $\Delta\varphi$-averaged radial distribution function, as in Fig. 2, and the integration is carried out over the first NN shell [23]; importantly, the quadratic power in the integrand makes ζ measure both the correlations and the anticorrelations with the same sign. Strikingly, the theoretical curve, which is roughly fourfold symmetric, significantly overestimates the strength of orientational correlations for $\Delta\varphi = 90°$, as shown on a polar plot in Fig. 4(b). This may support our hypothesis that the overestimate of orientational correlations by the PY model results into an underestimate of the positional correlations between the particles. Future studies should allow the full three-dimensional orientational correlations in our system to be measured and compared with the theoretical predictions, providing a baseline for a better understanding of these fundamental fluids.

We thank Dr. P. Pfleiderer, Professor J. Vermant, Mr. Y. Nemschitz, Dr. M. Schultz, and Mr. T. Freund, for their assistance with the particles' stretching process, Dr. P. J. Lu for his PLuTARC codes, and Dr. M. Letz for his PY code. The Kahn Foundation has generously funded part of the equipment used in this project. This research is supported by the Israel Science Foundation (No. 85/10, No. 1668/10).

*eli.sloutskin@biu.ac.il

[1] V. J. Anderson and H. N. W. Lekkerkerker, Nature (London) **416**, 811 (2002).
[2] J.-P. Hansen and I. R. McDonald, *Theory of Simple Liquids* (Elsevier, USA, 2006).
[3] J. K. Percus and G. J. Yevick, Phys. Rev. **110**, 1 (1958).
[4] P. H. Poole, F. Sciortino, U. Essmann, and H. E. Stanley, Nature (London) **360**, 324 (1992).
[5] A. Donev *et al.*, Science **303**, 990 (2004).
[6] D. Frenkel and B. M. Mulder, Mol. Phys. **55**, 1171 (1985).
[7] M. Letz and A. Latz, Phys. Rev. E **60**, 5865 (1999).
[8] C. De Michele, A. Scala, R. Schilling, and F. Sciortino, J. Chem. Phys. **124**, 104509 (2006).
[9] C. Baravian *et al.*, Europhys. Lett. **90**, 36005 (2010).
[10] Z. Zheng, F. Wang, and Y. Han, Phys. Rev. Lett. **107**, 065702 (2011).
[11] E. B. Mock and C. F. Zukoski, Langmuir **23**, 8760 (2007).

[12] A. Mohraz and M. J. Solomon, Langmuir **21**, 5298 (2005).
[13] Z. K. Zhang, P. Pfleiderer, A. B. Schofield, C. Clasen, and J. Vermant, J. Am. Chem. Soc. **133**, 392 (2011).
[14] AOT charges the particles, but also screens Coulombic interactions; thus, the Debye length in our solvent [G. S. Roberts *et al.*, Langmuir **24**, 6530 (2008)], free of particles, is ~ 0.3 μm. This charging may increase the effective size of our particles, beyond their hard size; thus, the particle size may have to be rescaled, when the experimental data are compared to theoretical models of hard particles.
[15] P. J. Lu, P. A. Sims, H. Oki, J. B. Macarthur, and D. A. Weitz, Opt. Express **15**, 8702 (2007).
[16] C. B. Barber, D. P. Dobkin, and H. Huhdanpaa, ACM Trans. Math. Softw. **22**, 469 (1996); www.qhull.org.
[17] R. Piazza, T. Bellini, and V. Degiorgio, Phys. Rev. Lett. **71**, 4267 (1993).
[18] G. Rickayzen, Mol. Phys. **95**, 393 (1998).
[19] J. Ram, R. C. Singh, and Y. Singh, Phys. Rev. E **49**, 5117 (1994).
[20] P. G. Ferreira, A. Perera, M. Morea, and M. M Telo da Gamma, J. Chem. Phys. **95**, 7591 (1991).
[21] J. Talbot, A. Perera, and G. N. Patey, Mol. Phys. **70**, 285 (1990).
[22] To obtain the PY-theoretical $g(r, \Delta\varphi)$, we average the full angle-dependent radial distribution function [7] $g(r, \theta_1, \theta_2, \varphi_1, \varphi_2)$ over θ_1, θ_2, and φ_1, under the condition that $\Delta\varphi = \varphi_2 - \varphi_2$. Inclusion of r^2 in ζ or f_z does not qualitatively change the result.
[23] Setting the range of integration in ζ to (b, r'), as in Fig. 4 (a) does not significantly change the result in Fig. 4(b). Importantly, as explained in the text, $g(r, 0)$ in the definition of f_z is different from (the $\Delta\varphi$-averaged) $g(r)$, which appears in the definition of ζ.